SUPPLEMENTARY INFORMATION AVAILABLE

Syntheses and Single Crystal X-Ray Diffraction Studies of Acyclic and Macrocyclic Aza-dithiolate (NS2) Complexes of (Arene)ruthenium(II). Thiolate-alkylation, Base-Promoted Hydroalkylation and Protonation Reactions.

Richard Y. C. Shin, Geok Kheng Tan, Lip Lin Koh and Lai Yoong Goh*
Department of Chemistry, National University of Singapore, Kent Ridge, Singapore 119260
E-mail: chmgohly@nus.edu.sg. Fax: (+65) 6779 1691

Table S1. Data Collection and Processing Parameters

complexes	(**2**)	(**3**)	(**5**)	(**6**)	(**7**)
formula	$C_{18}H_{30}N_2RuS_2$	$C_{19}H_{34}F_{12}N_2O_2P_2RuS_2$	$C_{22}H_{41}F_{12}N_3O_4P_2RuS_2$	$C_{19}H_{36}F_6IN_2O_2PRuS_2$	$C_{19}H_{32}F_6NPRuS_2$
M_r	439.63	777.61	866.71	761.56	584.62
temp, K	223(2)	223(2)	223(2)	223(2)	293(2)
cryst color and habit	red, cuboid	yellow, needle	yellow, orthorhombic	yellow, orthorhombic	red, orthorhombic
cryst size, mm^3	$0.30 \times 0.26 \times 0.12$	$0.14 \times 0.12 \times 0.10$	$0.50 \times 0.40 \times 0.24$	$0.38 \times 0.10 \times 0.04$	$0.20 \times 0.18 \times 0.08$
cryst system	Orthorhombic	Orthorhombic	Triclinic	Orthorhombic	Orthorhombic
space group	P2(1)2(1)2(1)	Pna2(1)	P-1	Pbca	Pbca
a, Å	9.7421(7)	17.7539(11)	10.1429(5)	16.9370(10)	10.0476(5)
b, Å	11.9068(8)	11.8517(8)	10.6403(5)	16.8727(10)	18.5151(9)
c, Å	16.4702(11)	13.7702(9)	16.5359(8)	19.7224(12)	24.9301(12)
α, deg	90	90	108.2100(10)	90	90
β, deg	90	90	98.1320(10)	90	90
γ, deg	90	90	93.9630(10)	90	90
V, $Å^3$	1910.5(2)	2897.4(3)	1665.96(14)	5636.1(6)	4637.8(4)
Z	4	4	2	8	8
density, g cm^{-3}	1.528	1.783	1.728	1.795	1.675
abs. coeff, mm^{-1}	1.040	0.895	0.793	1.916	0.980
F(000)	912	1568	880	3024	2384
θ range for data collection	2.11 to 30.05	2.07 to 27.49	2.03 to 27.50	1.99 to 25.00	1.63 to 27.50
index ranges	-13<=h<=12, -16<=k<=16, -19<=l<=22	-22<=h<=23, -15<=k<=15, -17<=l<=12	-13<=h<=13, -13<=k<=13, -21<=l<=21	-20<=h<=15, -19<=k<=20, -23<=l<=23	-13<=h<=9, -13<=k<=23, -32<=l<=29
no. of reflns collected	15629	19349	21453	30654	31086
indep reflns	5402	5086	7632	4948	5321
max. and min. transmission	0.863713 and 0.665252	0.9158 and 0.8849	0.8324 and 0.6924	0.9273 and 0.5297	0.9257 and 0.8281
no. of data/restraints/params	5402 / 0 / 219	5086 / 653 / 354	7632 / 694 / 604	4948 / 18 / 320	5321 / 0 / 405
final *R* indices [$I > 2\sigma(I)$] [a, b]	R1 = 0.0377, wR2 = 0.0845	R1 = 0.0475, wR2 = 0.1294	R1 = 0.0322, wR2 = 0.0885	R1 = 0.0583, wR2 = 0.1151	R1 = 0.0493, wR2 = 0.0992
R indices (all data)	R1 = 0.0408, wR2 = 0.0859	R1 = 0.0515, wR2 = 0.1330	R1 = 0.0337, wR2 = 0.0897	R1 = 0.0774, wR2 = 0.1221	R1 = 0.0611, wR2 = 0.1033
goodness-of-fit on F^2 [c]	1.080	1.038	1.035	1.138	1.197
large diff peak and hole, e $Å^{-3}$	0.894 and –0.688	0.838 and –0.548	0.629 and –0.592	0.809 and –1.230	1.037 and –1.098

[a] $R = (\Sigma||F_o| - |F_c||)\Sigma|F_o|$. [b] $wR_2 = [(\Sigma\omega(|F_o| - |F_c|)^2/\Sigma\omega|F_o|^2]^{1/2}$. [c] GoF $= [(\Sigma\omega(|F_o| - |F_c|)^2/(N_{obs}-N_{param})]^{1/2}$

Table S1 (contd). Data Collection and Processing Parameters

complexes	(**8**)	(**9**)	(**10**)	(**11**)	(**12**)
formula	$C_{22}H_{37}BrF_6N_1PRuS_2\{1.83(CH_3CN)\}$	$C_{20}H_{34}F_6NPRuS_2$	$C_{18}H_{30}F_6NPRuS_2$	$C_{18.50}H_{31.50}F_6N_{1.50}OPRuS_2$	$C_{20}H_{33.50}F_6N_{1.50}PRuS_2$
M_r	779.85	598.64	570.59	601.11	605.14
temp, K	223(2)	223(2)	223(2)	223(2)	223(2)
cryst color and habit	yellow, hexagonal	red, orthorhombic	red, cuboid	orange, orthorhombic	orange, orthorhombic
cryst size, mm^3	$0.36 \times 0.20 \times 0.10$	$0.20 \times 0.14 \times 0.12$	$0.46 \times 0.36 \times 0.22$	$0.15 \times 0.12 \times 0.10$	$0.30 \times 0.18 \times 0.14$
cryst system	Hexagonal	Monoclinic	Monoclinic	Monoclinic	Monoclinic
space group	P6(3)/m	P2(1)/c	P2(1)/n	P2(1)/c	P2(1)/c
a, Å	16.7659(5)	8.9741(5)	12.3846(7)	17.947(3)	18.3830(9)
b, Å	16.7659(5)	16.8112(9)	13.8429(7)	21.283(4)	21.1216(11)
c, Å	45.705(3)	15.8708(8)	13.7618(8)	12.559(2)	12.5607(6)
α, deg	90	90	90	90	90
β, deg	90	92.5870(10)	107.0470(10)	102.396(4)	101.8320(10)
γ, deg	120	90	90	90	90
V, $Å^3$	11126.3(8)	2391.9(2)	2255.6(2)	4685.5(14)	4773.4(4)
Z	12	4	4	8	8
density, g cm^{-3}	1.795	1.662	1.680	1.704	1.684
abs. coeff, mm^{-1}	1.704	0.952	1.005	0.976	0.956
$F(000)$	4744	1224	1160	2448	2472
θ range for data collection	1.66 to 24.00	1.77 to 27.50	1.95 to 30.01	1.50 to 25.00	1.13 to 25.00
index ranges	-17<=h<=19, -19<=k<=17, -46<=l<=52	-11<=h<=7, -21<=k<=21, -20<=l<=20	-14<=h<=17, -13<=k<=19, -18<=l<=19	-21<=h<=10, -25<=k<=25, -14<=l<=14	-21<=h<=21, -25<=k<=25, -14<=l<=14
no. of reflns collected	59241	16640	18088	25908	27372
indep reflns	5914	5492	6408	8258	8382
max. and min. transmission	0.8481 and 0.5790	0.8943 and 0.8324	0.8091 and 0.6549	0.9087 and 0.8674	0.8778 and 0.7625
no. of data/restraints/params	5914 / 102 / 373	5492 / 13 / 314	6408 / 357 / 326	8258 / 771 / 616	8382 / 2 / 599
final R indices $[I > 2\sigma(I)]$ [a, b]	R1 = 0.1325, wR2 = 0.3183	R1 = 0.0399, wR2 = 0.0956	R1 = 0.0367, wR2 = 0.0904	R1 = 0.0737, wR2 = 0.1424	R1 = 0.0558, wR2 = 0.1189
R indices (all data)	R1 = 0.1637, wR2 = 0.3342	R1 = 0.0505, wR2 = 0.1000	R1 = 0.0437, wR2 = 0.0944	R1 = 0.1236, wR2 = 0.1585	R1 = 0.0739, wR2 = 0.1309
goodness-of-fit on F^2 [c]	1.102	1.042	1.043	1.059	1.092
large diff peak and hole, e $Å^{-3}$	2.360 and –1.613	0.909 and –403	0.926 and –0.310	1.416 and –1.052	0.919 and –653

[a] $R = (\Sigma||F_o| - |F_c||)\Sigma|F_o|$. [b] $wR_2 = [(\Sigma\omega||F_o| - |F_c|)^2/\Sigma\omega|F_o|^2]^{1/2}$. [c] GoF $= [(\Sigma\omega||F_o| - |F_c|)^2/(N_{obs}-N_{param})]^{1/2}$

Table S2. IR spectral data[a]

Complex	υ (cm^{-1})
2	3160 s (N–H), 3007 w, 2960 msh, 2903 s, 2848 msh, 1442 s, 1384 s, 1286 w, 1268 w, 1237m, 1217 w, 1189 w, 1104 s, 1068 s, 1018 s, 956 s, 908 m, 794 m, 675 w, 651 w, 551 w.
3	3294 m (N–H), 3232 m, 3059 m, 2964 m, 2934 m, 2879 m, 1459 s, 1419 s, 1396 m, 1288 m, 1255 m, 1222 w, 1124 m, 1073 m, 1014 m, 975 m, 847 vs (PF_6), 741 m, 558 s (PF_6).
4	3291 m (N–H), 2988 broad m, 1458 m, 1420 m, 1395 m, 1290 w, 1214 w, 1105 w, 1071 m, 1027 w, 970 w, 845 vs (PF_6), 740 w, 653 w, 558 s (PF_6).
5	3291 m (N–H), 2935 w, 2875 w, 1449 m, 1416 m, 1393 m, 1290 m, 1253 w, 1229 w, 1209 w, 1145 w, 1108 w, 1070 m, 1013 m, 965 m, 845 vs (PF_6), 740 m, 656 w, 558 s (PF_6).
6	3655 m, 3577 m, 3307 w (N–H), 3096 m, 2995 w, 2923 w, 1452 m, 1396 m, 1321 w, 1291 w, 1223 w, 1116 w, 1073 m, 1026 m, 995 m, 958 m, 842 vs (PF_6), 740 w, 558 s (PF_6).
7	3291 m (N–H), 3084 w, 2979 w, 2919 w, 2868 w, 1449 m, 1412 m, 1389 m, 1292 w, 1242 w, 1220 w, 1098 w, 1069 w, 1008 w, 968 w, 920 w, 845 vs (PF_6), 739 w, 669 w, 558 s (PF_6).
8	3036 w, 2934 w, 2878 w, 2800 w, 1452 w, 1393 w, 1296 vw, 1125 w, 1070 w, 1018 w, 960 w, 930 w, 843 s (PF_6), 739 w, 557 m (PF_6).
9	3292 m (N–H), 2973 w, 2929 m, 2869 w, 1447 m, 1390 m, 1290 w, 1220 w, 1138 w, 1069 m, 1013 m, 967 m, 926 m, 841 vs (PF_6), 739 m, 558 s (PF_6).
10	3308 m (N–H), 2923 w, 2869 w, 1450 m, 1389 m, 1298 w, 1260 w, 1212 w, 1068 m, 1021 m, 966 m, 840 vs (PF_6), 774 w, 740 w, 609 w, 558 s (PF_6).
11	3309 m (N–H), 2952 msh, 2937 m, 2891 wsh, 1448 m, 1388 m, 1329 w, 1301 w, 1244 w, 1216 w, 1093 w, 1055 m, 1043 m, 978 w, 914 msh, 836 vvs (PF_6), 765 w, 740 w, 681 w, 558 s (PF_6).

12	3309 w (N–H), 2964 wsh, 2928 m, 2888 wsh, 1451 m, 1393 m, 1300 w, 1248 w, 1212 w, 1140 w, 1069 w, 1015 w, 978 w, 842 vs (PF_6), 763 w, 675 w, 558 s (PF_6).

[a] KBr pellet

Table S3. Selected Bond Lengths (Å) and Angles (deg) of complexes

complex	**3**	**A**[#]	**5**	**B**[##]
Ru(1)–S(1)	2.327(2)	2.323(2)	2.3401(6)	2.3341(13)
Ru(1)–S(2)	2.3175(16)	2.320(2)	2.3320(6)	2.3151(13)
Ru(1)–N(1)	2.153(6)	2.329(2)	2.158(2)	2.3410(13)
S(1)–Ru(1)–S(2)	87.21(7)	87.28(9)	99.08(2)	98.47(5)
S(1)–Ru(1)–N(1)	82.9(2)	87.05(9)	82.77(6)	86.89(5)
S(2)–Ru(1)–N(1)	83.62(18)	86.75(9)	83.72(6)	85.45(5)

[#] **A =** 9S3 analogue of **3,** i.e. $[(HMB)Ru(9S3)]^{2+}$.[1] [##] **B** = 11S3 analogue of **5**.[1]

Table S4. Selected Bond Lengths (Å) and Angles (deg) of complexes

complex	**1**[1]	**2**	**6**	**11**		**12**	
				a [#]	**b** [#]	**a** [#]	**b** [#]
Ru(1)–S(1)	2.3807(10)	2.3786(9)	2.3480(17)	2.385(2)	2.387(2)	2.3817(15)	2.3880(15)
Ru(1)–S(2)	2.3851(10)	2.3844(9)	2.3394(19)	2.343(2)	2.333(2)	2.3270(16)	2.3303(16)
Ru(1)–N(1)	2.3396(10)	2.161(3)	2.147(6)	2.160(7)	2.151(7)	2.141(5)	2.148(4)
S(2)–C(5)	-	-	-	1.833(11)	1.803(9)	1.873(8)	1.826(7)
C(5)–C(6)	-	-	-	1.478(15)	1.525(13)	1.489(10)	1.490(9)
C(6)–C(13)	-	-	-	1.573(13)	1.544(12)	-	-
C(13)–C(7)	-	-	-	1.522(12)	1.517(11)	-	-
C(6)–C(14)	-	-	-	-	-	1.513(9)	1.546(8)
C(14)–C(8)	-	-	-	-	-	1.523(8)	1.513(8)
S(1)–Ru(1)–S(2)	92.18(4)	89.87(4)	102.93(6)	84.39(10)	85.00(8)	84.26(6)	83.89(6)
S(1)–Ru(1)–N(1)	85.18(4)	82.11(9)	82.85(18)	82.6(2)	82.1(2)	82.85(16)	83.26(13)
S(2)–Ru(1)–N(1)	85.41(4)	83.55(9)	82.67(18)	84.1(2)	84.1(2)	83.84(16)	84.06(14)

[#] **a** and **b** are two independent molecules in the unit cell.

Table S5. Selected Bond Lengths (Å) and Angles (deg) of complexes

complex	**10**	**7**	**8**	**9**	**C**[#]
Ru(1)–S(1)	2.3708(7)	2.3809(9)	2.343(6)	2.3777(8)	2.374(2)
Ru(1)–S(2)	2.3500(7)	2.3303(10)	2.353(5)	2.3345(8)	2.346(2)
Ru(1)–N(1)	2.154(2)	2.145(3)	2.174(15)	2.156(3)	2.320(2)
S(1)–C(1)	1.825(3)	1.819(5)	1.80(2)	1.843(4)	1.86(2)
S(1)–C(5)	-	-	1.862(19)	-	-
S(2)–C(3)	-	-	1.82(2)	-	-
S(2)–C(4)	-	1.805(5)	-	1.822(5)	-
S(2)–C(5)	1.756(4)	1.818(5)	-	1.828(4)	1.77(1)
S(2)–C(8)	-	-	1.829(19)	-	-
C(5)–C(6)	1.304(6)	1.461(9)/1.578(19)	1.49(3)	1.507(6)	1.25(1)
C(6)–C(7)	-	1.270(15)	1.26(4)	1.499(7)	-
C(7)–C(8)	-	-	-	1.296(8)/1.25(2)	-
C(8)–C(9)	-	-	1.45(3)	-	-
C(9)–C(10)	-	-	1.31(4)	-	-
S(1)–Ru(1)–S(2)	91.04(3)	95.27(4)	104.39(19)	94.10(3)	90.04(7)
S(1)–Ru(1)–N(1)	81.40(7)	80.27(9)	84.4(5)	82.23(8)	85.17(7)
S(2)–Ru(1)–N(1)	82.44(7)	83.98(9)	82.0(5)	82.98(8)	85.93(7)
Ru(1)–S(2)–C(5)	109.86(15)	115.81(19)	121.4(8)[##]	116.06(14)	112.3(4)
Ru(1)–S(1)–C(1)	101.26(11)	101.94(15)	98.7(8)	94.70(15)	103.2(6)
Ru(1)–S(1)–C(5)	-	-	119.2(8)	-	-
Ru(1)–S(2)–C(3)	-	-	102.7(7)	-	-
Ru(1)–S(2)–C(4)	98.70(11)	98.18(16)	-	102.56(16)	104.3(3)
Ru(1)–S(2)–C(8)	-	-	121.4(8)	-	-

[#] **C** = 'S3' analogue of **10**.[20] [##] for Ru(1)–S(2)–C(8)

Figure S1. ORTEP plots for the molecular structures of (a) **2** and (b) **3** dication. Thermal ellipsoids are drawn to 50 % probability level. Hydrogen atoms are omitted for clarity.

(a) (b)

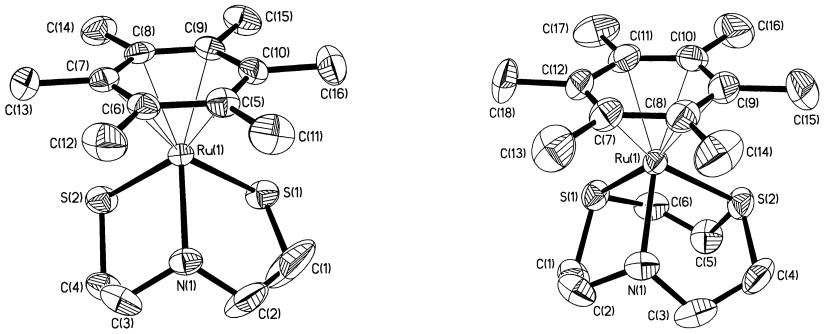

Figure S2. ORTEP plots for the molecular structures of (a) dicationic bis(SMe) complex **6**, and monocationic (b) S-allyl complex **7** and (c) S-vinyl complex **10**. Thermal ellipsoids are drawn to 50 % probability level. Hydrogen atoms are omitted for clarity.

(a) (b)

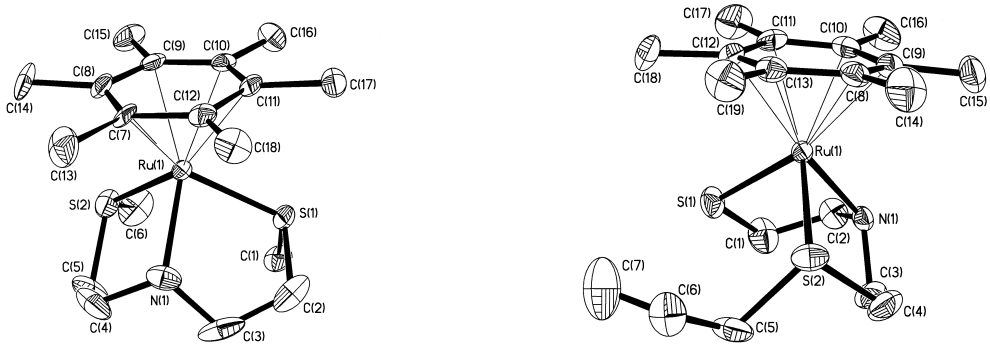

(c)

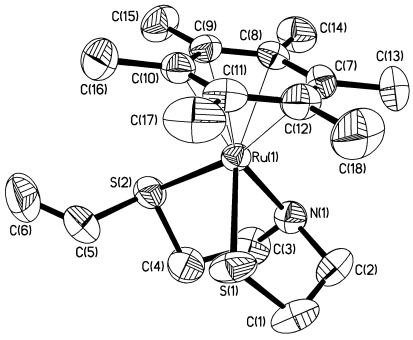

Figure S3: ^{1}H NMR spectra of **10** in CD_3CN before and after protonation (a) vinylic region and (b) "aliphatic Region"

(a) vinylic region (peak intensities are magnified relative to those in region (b))

(b) " aliphatic region"

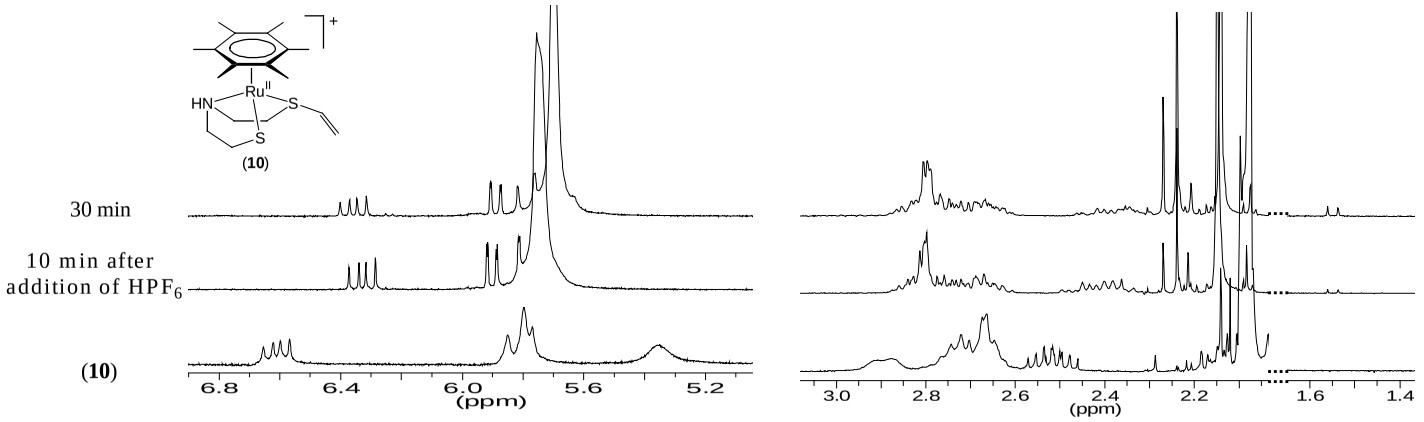

Figure S4: ^{1}H-NMR spectra of **7** in CD_3CN before and after protonation

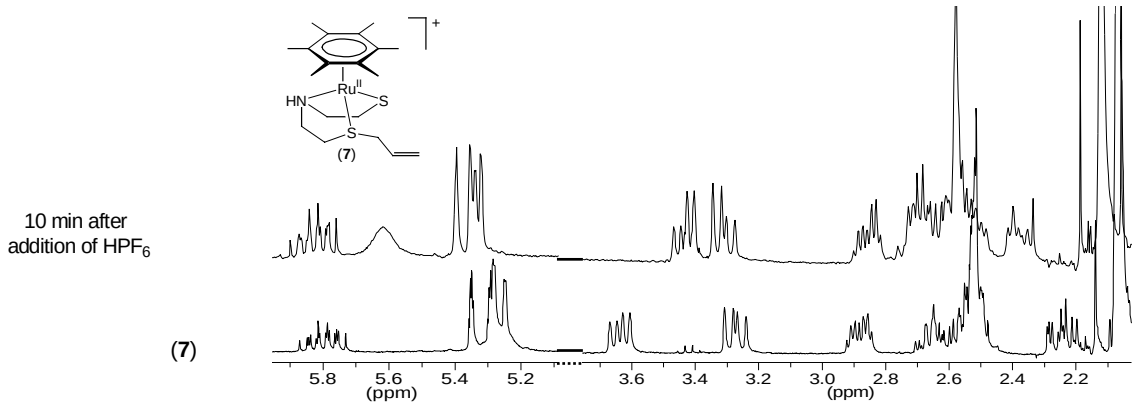

Protonation of **7** initiated an immediate disappearance of its arene Me resonance (δ 2.07), which was replaced by a new Me resonance at δ 2.12, a slight shift in resonances assigned to the vinylic protons, i.e. the 14-line multiplet for S…C*H*= to δ 5.90–5.76, and the 4-line mutiplet to δ 5.39–5.32 (unres dd ≡ apparent d, J = 11.4 Hz, =CH_2), δ 5.33 (unres dd ≡ apparent d, J = 4.1 Hz, =CH_2); multiplets for SCH_2/$HNCH_2$'s are significantly different in chemical shifts and coupling fine structure from those for **7**, and are found at δ 3.47–3.28 (symm 8-line, 2H), δ 2.90 – 2.76 (overlapping quartets, 1H), δ 2.76–2.45 (unsymm, 6H), δ 2.41–2.34 (unsymm, 1H) and δ 1.43–1.27 (unsymm, 1H); the S–H resonance is obscured under these multiplets and could not be definitively identified from amongst the component peaks.

Figure S5: ^{1}H-NMR spectra of **9** in CD_3CN before and after protonation

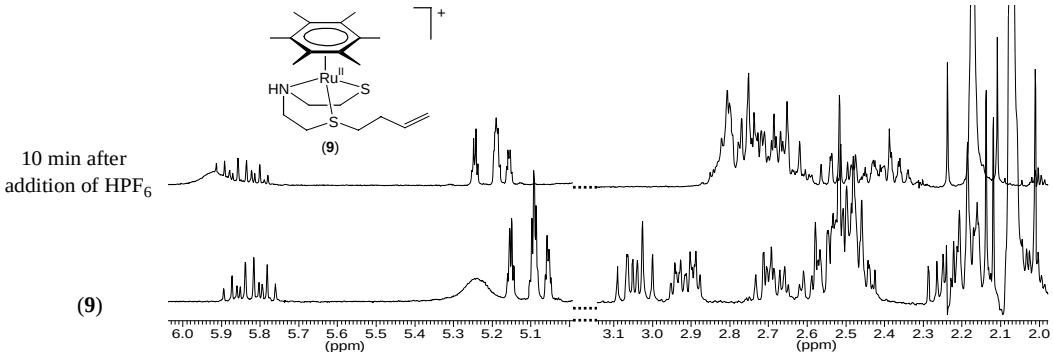

Instantaneous changes were observed in the ^{1}H NMR spectrum of **9** upon protonation, viz. the immediate replacement of its arene Me resonance (δ 2.07) with a new Me resonance at δ 2.17 and a shift of δ(NH) from 5.24 to 5.92. The new vinylic proton resonance possesses a very similar coupling pattern to that in **9**, but is shifted to δ 5.85 (10-line m ≡ tdd (*J* 17.2, 10.4, 6.4 Hz), 1H, $SCH_2CH_2C\mathit{H}=$) and 5.22 (quartet-like ≡ partially res. tdd (*J* = 18.1, ca. 2, 1.6 Hz), 1H, $\mathit{CH}H=CHCH_2CH_2S$), 5.17 (quartet-like tdd, (*J* = 10.8, ca.2, 1.2 Hz), 1H, $C\mathit{H}H=CHCH_2CH_2S$); the multiplets belonging to the $SCH_2/HNCH_2$'s are significantly different in coupling patterns, being found as highly unsymmetrical sets in the range δ 2.81–2.59 (10H) and δ 2 57–2.31 (3H).

Experimental Section

General procedures. Standard procedures were as described in a previous paper.[1] The compound $[(HMB)RuCl_2]_2$[2] and the ligand $HN(CH_2CH_2SH)_2$[3] were prepared as reported in the literature. Other reagents were obtained commercially.

1. Shin, R. Y. C.; Bennett, M. A.; Goh, L. Y.; Chen, W.; Hockless, D. C. R.; Leong, W. K.; Mashima, K.; Willis, A. C. *Inorg. Chem.* **2003**, *42*, 96.
2. Bennett, M. A.; Huang, T.-N.; Matheson, T. W.; Smith, A. K. *Inorg. Synth.* **1982**, *21*, 74.
3. Rima, G.; Satgé, J.; Fatome, M.; Laval, J. D.; Sentenac-Roumanou, H.; Lion, C.; Lazraq, M. *Eur. J. Med. Chem.* **1991**, *26*, 291.

Reactions of 2 with haloalkanes. *With dibromoalkanes.* Complex [(HMB)Ru{η^3-$S(CH_2)_2NH(CH_2)_2S(CH_2)_3$}]$(PF_6)_2$ (**4**) was similarly obtained as yellow crystalline plates (42 mg, 76% yield) from the reaction of **2** (30 mg, 0.075 mmol) with $Br(CH_2)_3Br$ (75 μL, 0.74 mmol). ^{1}H NMR (δ, CD_3CN): N*H*: 6.02 (br s, 1H); SCH_2 + HNCH_2: 2.97–2.61 (28-line m, 12H), 2.41–2.27 (13-line m, 1H), 1.89–1.77 (12-line m, 1H); C_6Me_6: 2.18 (s, 18H). ^{13}C NMR (δ, CD_3CN): C_6Me_6: 103.6; HNCH_2: 54.4; SCH_2: 36.1, 29.5, 24.6; C_6Me_6: 15.6. IR (ν cm^{-1}, KBr): 3291 m (N–H), 845 vs and 558 s (PF_6). FAB$^+$ MS: *m/z* 586 $[M - PF_6]^+$, 440 $[M - 2PF_6 - 1]^+$, 366 $[M - 2PF_6 - S(CH_2)_2NH]^+$, 335 $[M - 2PF_6 - S_2(CH_2)_2NH + 1]^+$. FAB$^-$ MS: *m/z* 145. Anal. Found: C, 31.2; H, 4.5; N, 2.3; P, 7.9; S, 9.1. Calcd for $C_{19}H_{33}F_{12}NP_2RuS_2$: C, 31.2; H, 4.6; N, 1.9; P, 8.5; S, 8.8.

Complex [(HMB)Ru{η^3-$S(CH_2)_2NH(CH_2)_2S(CH_2)_4$}]$(PF_6)_2$ (**5**) was also obtained as yellow crystalline plates (29 mg, 78% yield) from the reaction of **2** (20 mg, 0.050 mmol) with $Br(CH_2)_4Br$ (40 μL, 0.33 mmol). ^{1}H NMR (δ, CD_3CN): N*H*: 5.99 (br s, 1H); SCH_2 + HNCH_2: 3.31–3.24 (4-line m, 2H), 2.78 (m, 8H), 2.37–2.26 (5-line m, 2H), 2.05 (c.unres.m, 2H), 1.45 (c.unres.m, 2H); C_6Me_6: 2.16 (s, 18H). ^{13}C NMR (δ, CD_3CN): C_6Me_6: 103.1; HNCH_2: 52.1; SCH_2: 38.4, 33.3, 25.0; C_6Me_6: 15.6. IR (ν cm^{-1}, KBr): 3291 m (N–H), 845 vs and 558 s (PF_6). FAB$^+$ MS: *m/z* 600 $[M - PF_6]^+$, 454 $[M - 2PF_6 - 1]^+$, 366 $[M - 2PF_6 - S(CH_2)_3NH]^+$. FAB$^-$ MS: *m/z* 145. Anal. Found: C, 31.8; H, 4.8; N, 2.7; P, 8.0; S, 8.9. Calcd for $C_{20}H_{35}F_{12}NP_2RuS_2$: C, 32.3; H, 4.7; N, 1.9; P, 8.3; S, 8.6.

With iodomethane. Into a stirred solution of **2** (18 mg, 0.045 mmol) in MeOH (10 mL) was injected MeI (28 μL, 0.45 mmol). The solution was stirred for 48 h, resulting in a gradual color change from red to yellow. Metathesis with NH_4PF_6 (40 mg, 0.24 mmol) led to precipitation of the product as yellow solids together with NH_4I. Filtration and subsequent workup yielded yellow crystalline solids of [(HMB)Ru{η^3-$NH(CH_2CH_2SMe)_2$}](I.PF_6) (**6**) (20 mg, 63% yield) from CH_3NO_2-ether after 24 h at –30 °C. ^{1}H NMR (δ, CD_3CN): N*H*: 6.51 (br s, 1H); SCH_2 + HNCH_2: 2.92–2.71 (m, 6H), 2.65–2.57 (unres m, 2H); SCH_3: 2.33 (s, 6H); C_6Me_6: 2.19 (s, 18H). ^{13}C NMR (δ, CD_3CN): C_6Me_6: 103.0; HNCH_2: 52.9; SCH_2: 38.1; SCH_3: 21.2; C_6Me_6: 16.1. IR (ν cm^{-1}, KBr): 3307 w (N–H), 842 vs and 558 s (PF_6). FAB$^+$ MS: *m/z* 574 $[M - I]^+$, 556 $[M - PF_6]^+$, 428 $[M - I - PF_6 - H]^+$, 414 $[M - I - PF_6 - CH_3]^+$. FAB$^-$ MS: *m/z* 145. Anal. Found: C, 30.6; H, 5.0; N, 2.0; S, 9.0. Calcd for $C_{18}H_{33}F_6INPRuS_2$: C, 30.9; H, 4.8; N, 2.0; S, 9.2.

Reactions of 2 with bromoalkenes.

With excess allyl bromide. Into a stirred solution of **2** (30 mg, 0.075 mmol) in MeOH (8 mL) was injected CH_2=$CHCH_2Br$ (34 μL, 0.40 mmol). The solution gradually changed from red to yellow over a period of 12 h. Metathesis with NH_4PF_6 (50 mg, 0.30 mmol) followed by the usual workup procedures gave a yellow oil (48 mg), which after trituration with THF (8 mL) to extract out a minor uncharacterizable yellow component, was found to possess a ^{1}H NMR spectrum indicating the presence of mainly [(HMB)Ru{η^3-$NH((CH_2)_2SCH_2CH=CH_2)_2$}](Br.$PF_6$) (**8**) (ca. 90% yield), together with trace amounts of two other arene-containing impurity complex which also carried a S-allylic substituent. This was very difficult to purify and crystallize. After several attempts some yellow crystalline plates of (**8**) (8 mg, 16% yield) were successfully obtained from a CH_3CN-ether solution after 3 days at –30 °C. ^{1}H NMR (δ, CD_3CN): N*H*: 7.92 (br s, 1H); SCH_2CH=: 6.03–5.90 (symm 14-line m, 2H); =$CH_{trans}H$: 5.50 (d, J = 16.9 Hz, 2H); =$CH_{cis}H$: 5.42 (d, J = 10.1 Hz, 2H); SCH_2 + $HNCH_2$: 3.40–3.33 (4-line m, 2H), 3.26–3.19 (4-line m, 2H), 2.93–2.83 (unres m, 2H), 2.77–2.63 (unres m, 6H); C_6Me_6: 2.24 (s, 18H). ^{13}C NMR (δ, CD_3CN): *C*H=: 130.8; =CH_2: 123.4; C_6Me_6: 103.3; $HNCH_2$: 52.9; SCH_2: 41.2, 35.0; C_6Me_6: 15.8. IR (ν cm^{-1}, KBr): 843 vs and 557 s (PF_6). FAB$^+$ MS: *m/z* 626 [M – Br]$^+$, 562 [M – PF_6]$^+$, 480 [M – Br – PF_6 – H]$^+$, 440 [M – Br – PF_6 – $CH_2CH=CH_2$]$^+$, 399 [M – Br – PF_6 – $(CH_2CH=CH_2)_2$]$^+$. FAB$^-$ MS: *m/z* 145. Anal. Found: C, 37.4; H, 5.4; N, 2.2; S, 9.1. Calcd for $C_{22}H_{37}BrF_6NPRuS_2$: C, 37.5; H, 5.3; N, 2.0; S, 9.1.

With 4-bromobutene. Into a stirred solution of **2** (100 mg, 0.25 mmol) in MeOH (15 mL) was injected CH_2=$CH(CH_2)_2Br$ (38 μL, 0.37 mmol). The solution was stirred for 2 h and then evacuated to dryness to remove excess 4-bromobutene. The red residue was redissolved in MeOH and NH_4PF_6 (200 mg, 1.22 mmol) added. After stirring for 30 min, the solution was evacuated to dryness and the product extracted with CH_3CN (3 × 3 mL). The red extracts were passed through a disk of alumina (Act III, 1.5 cm) giving two red bands. The first band gave deep red crystals of [(HMB)Ru{η^3-$S(CH_2)_2NH(CH_2)_2S(CH_2)_2CH=CH_2$}]$PF_6$ (**9**) (105 mg, 82% yield based on reacted **2**) upon recrystallization in ether for 1 day at –30 °C. The second fraction gave red crystals of the starting substrate **2** (14 mg, 0.035 mmol, 14% recovery) upon recrystallization with ether. For **9**: ^{1}H NMR (δ, CD_3CN): $S(CH_2)_2CH$=: 5.83 (10-line m ≡ tdd (*J* = 16.9, 10.4, 6.4 Hz), 1H); N*H*: 5.24 (s br, 1H); $CH_{trans}H$=$CH(CH_2)_2S$: 5.12 (quartet-like ≡ partially res. tdd (*J* = 18.1, ca. 2, 1.6 Hz), 1H); $CH_{cis}H$=$CH(CH_2)_2S$: 5.07

(quartet-like tdd, (J = 10.8, ca.2, 1.2 Hz), 1H); SCH_2 + HNCH_2: 3.09–3.00 (symm 6-line m, 1H), 2.95–2.88 (symm 7-line m, 1H), 2.73–2.61 (unsymm 10-line m, 1H), 2.59–2.42 (unsymm 12-line m, 6H), 2.29–2.16 (unsymm 10-line m, 3H); C_6Me_6: 2.07 (s, 18H). ^{13}C NMR (δ, CD_3CN): *C*H=: 136.5; =*C*H_2: 117.0; *C*$_6$Me$_6$: 97.9; HN*C*H_2: 60.5, 50.4; S*C*H_2 and SCH$_2$*C*H_2: 38.2, 32.3, 31.7, 26.7; C_6Me_6: 15.4. IR (ν cm^{-1}, KBr): 3292 m (N–H), 841 vs and 558 s (PF_6). FAB$^+$ MS: *m/z* 454 [M – PF_6]$^+$, 399 [M – PF_6 – $(CH_2)_2CH{=}CH_2$]$^+$, 352 [M – PF_6 – $(CH_2)_2CH{=}CH_2$ – SCH_2 – H]$^+$. FAB$^-$ MS: *m/z* 145. Anal. Found: C, 40.3; H, 5.9; N, 2.8; S, 11.0. Calcd for $C_{20}H_{34}F_6NPRuS_2$: C, 40.1; H, 5.7; N, 2.3; S, 10.7.

Reactions with base.

*Reaction of **3** with one mol equivalent of KOH*. A solution of **3** (25 mg, 0.035 mmol) in CH_3CN (5 mL) was stirred with solid KOH (2 mg, 0.036 mmol) for 1 h resulting in a color change from pale yellow to reddish orange. The product suspension was filtered through a disk of Celite and the filtrate concentrated to ca. 3 mL and ether added. Yellow crystalline plates of **3** (5 mg, 20%) were recovered on cooling to –30 °C for 12 h. Addition of more ether to the red mother liquor gave red crystals of [(HMB)Ru{η^3-$S(CH_2)_2NH(CH_2)_2SCH{=}CH_2$)}]$PF_6$ (**10**) (10 mg, 63% yield based on reacted **3**) after 2 days at –30 °C.

*Reaction of **3** with excess KOH or KOBu^t*. Into a solution of **3** (16 mg, 0.022 mmol) in CH_3CN (3 mL) was added KOH (5 mg, 0.089 mmol) (or KOBu^t 8 mg, 0.036 mmol) and the solution was stirred for 3 h or 1 h (for KOBu^t), resulting in a color change from pale yellow through reddish orange to orange. The solution was filtered through a disk of Celite (1.5 cm), and the filtrate concentrated to ca. 2 mL. Addition of ether gave orange needle-shaped crystals of [Ru{η^6:η^3-$C_6Me_5(CH_2)_3S(CH_2)_2NH(CH_2)_2S$}]$PF_6$ (**11**) (12 mg, 99% yield) after 2 days at –30 °C. ^{1}H NMR (δ, CD_2Cl_2): N*H*: 5.23 (br s, 1H); SCH_2 + HNCH_2: 3.01–2.94 (12-line m, 1H), 2.85–2.72 (12-line m, 2H), 2.70–2.59 (unsymm m, 6H), 2.57–2.46 (7-line m, 1H), 2.44–2.36 (8-line m, 1H), 2.31–2.23 (13-line m, 1H), 2.12–2.07 (m, partly obscured by the C_6Me_5 peak, 1H), 2.04–1.97 (m, also partly obscured by the C_6Me_5 peak, 1H); C_6Me_5: 2.21, 2.18, 2.10, 2.03, 1.95 (each s, 15 H). ^{13}C NMR (δ, CD_3CN): *C*$_6$Me$_5$: 100.1 (overlapping peaks), 97.4, 96.7, 96.3, 87.5; HN*C*H_2: 63.5, 54.7; S*C*H_2: 38.7, 31.8, 27.9, 27.4, 24.3; C_6Me_5: 16.9, 16.0 and 15.6 (overlapping s), 14.8. IR ν (cm^{-1}, KBr): 3309 m (N–H), 836 vvs and 558 s (PF_6). FAB$^+$ MS: *m/z* 426 [M – PF_6]$^+$, 379 [M – PF_6 – SNH]$^+$, 323 [M – PF_6 –

$S(CH_2)_4NH]^+$. FAB^- MS: *m/z* 145. Anal. Found: C, 37.6; H, 5.2; N, 2.5; S, 11.2. Calcd for $C_{18}H_{30}F_6NPRuS_2$: C, 37.9; H, 5.3; N, 2.5; S, 11.2.

Similar treatment of **4** and **5** with KOH in CD_3CN caused a color change to orange, accompanied by disappearance of the NH proton resonance in the ^1H NMR spectrum and significant decrease in resolution of all the peaks which are also slightly upfield-shifted. An attempt to isolate the product from the reaction of **4** led to recovery of the starting complex.

*Reaction of **7** with KOH.* Into a stirred solution of **7** (21 mg, 0.036 mmol) in CH_3CN (5 mL) was added KOH (2 mg, 0.036 mmol). The solution immediately changed from red to dark blue and gradually to orange over 15 h. A ^1H NMR spectrum of this intermediate dark blue species showed broad peaks and an isolation attempt proved futile as the species was obviously undergoing further transformation. The final orange solution was filtered and the filtrate was passed through a disk of alumina (1.5 cm, ACT III), and eluted out with CH_3CN. From the orange eluate was obtained an oil residue. Recrystallization in THF-ether gave orange crystalline solids of $[Ru\{\eta^6:\eta^3\text{-}C_6Me_5CH_2CH(Me)CH_2S(CH_2)_2NH(CH_2)_2S\}]PF_6$ (**12**) (16 mg, 76 %) after 1 day at –30 °C.

Protonation with HPF_6: Into a CD_3CN (0.5 mL) solution of **7** (5 mg, 0.0086 mmol) in an NMR tube, cooled to 0°C, was injected 1.5 mol equivalents of dilute HPF_6 (200 μL, 0.068 M prepared by diluting 60% HPF_6 in CD_3CN). An immediate color change from reddish orange to pale orange was observed. The ^1H NMR spectra of the solution were monitored at intervals (10, 60, 180 min, daily up to 4 days). Similar protonation studies were done on complexes **9** (5 mg and 150 μL of the above diluted HPF_6) and **10** (4 mg and 150 μL of the above diluted HPF_6).

Attempts were made to isolate the protonated products of **7** and **9.** However, upon workup by concentration and addition of hexane or ether, the products readily reverted to the original complexes.

Crystal Structure Determinations. The crystals were mounted on glass fibers. X-ray data were collected on a Bruker AXS SMART APEX CCD diffractometer, using Mo-K_α radiation (λ = 0.71073 Å) at 223 K. The program SMART[4] was used for collecting the intensity data, indexing and determination of lattice parameters, SAINT[4] was used for integration of the intensity of reflections and scaling, SADABS[5] was used for absorption correction and SHELXTL[6] for space group and structure determination and least-squares refinements against F^2. The structures were solved by direct methods to locate the heavy atoms, followed by difference maps for the light, non-hydrogen atoms. The hydrogens were placed in calculated positions. Fluorine atoms of the PF_6^- anions of **3**, **5**, **10** and **11** were disordered. The ethylene carbons (C6 and C7) in **7**, the propyl group and the two bridging –C_2H_4– groups in **9** were disordered. In one of the cations of **12** the carbon C5 is disordered into two positions of 70% and 30% occupancy. There is one nitromethane molecule present per asymmetric unit, as space filling solvent in complexes **3**, **6** and **11**, and two such solvent molecules in **5.** Similarly there is one acetonitrile molecule per asymmetric unit in complexes **2** and **12.** The quality of X-ray data for complex **8** was bad (high Rint of 0.1649), due to the poor quality of the crystal, resulting from rapid loss of lattice acetonitrile from which it was crystallized under diffusion of ether. Hence data collection was difficult and the set of data used was the best that was obtained. The final R1 and wR2 values were relatively high. However, despite the poor R values, the structure of the cation could be confirmed. After the atoms of the cation and anion were located, there were residual peaks in some of the voids. These were fitted with acetonitrile molecules, one of which was given a one-third occupancy (resulting in 1.83 CH_3CN in the formula). Crystal data collection and processing parameters are given in Table S1.

4. SMART & SAINT Software Reference manuals, version 5.0, Bruker AXS Inc., Madison, WI, **1998**.
5. Sheldrick, G.M. SADABS software for empirical absorption correction; University of Göttingen: Germany, **2000**.
6. SHELXTL Reference Manual, version 5.1, Bruker AXS Inc., Madison, WI, **1998**.
